CSIRO PUBLISHING

International Journal of Wildland Fire **2017**, *26*, 296–305
http://dx.doi.org/10.1071/WF16128

Emissions of forest floor and mineral soil carbon, nitrogen and mercury pools and relationships with fire severity for the Pagami Creek Fire in the Boreal Forest of northern Minnesota

Randall K. Kolka[A,H], *Brian R. Sturtevant*[B], *Jessica R. Miesel*[C], *Aditya Singh*[D], *Peter T. Wolter*[E], *Shawn Fraver*[F], *Thomas M. DeSutter*[G] *and Phil A. Townsend*[D]

[A]USDA Forest Service, Northern Research Station, 1831 Highway 169 East, Grand Rapids, MN 55744, USA.
[B]USDA Forest Service, Northern Research Station, 5985 Highway K, Rhinelander, WI 54501, USA.
[C]Michigan State University, Department of Forestry, 480 Wilson Road, East Lansing, MI 48824, USA.
[D]University of Wisconsin Madison, Department of Forest and Wildlife Ecology, 1630 Linden Drive, Madison, WI 53706, USA.
[E]Iowa State University, Department of Natural Resource Ecology and Management, 333 Science II, Ames, IA 50011, USA.
[F]University of Maine, School of Forest Resources, 5755 Nutting Hall, Orono, ME 04469, USA.
[G]North Dakota State University, Department of Soil Science, Walster Hall 106, Fargo, ND 58108, USA.
[H]Corresponding author. Email: rkolka@fs.fed.us

Abstract. Forest fires cause large emissions of C (carbon), N (nitrogen) and Hg (mercury) to the atmosphere and thus have important implications for global warming (e.g. via CO_2 and N_2O emissions), anthropogenic fertilisation of natural ecosystems (e.g. via N deposition), and bioaccumulation of harmful metals in aquatic and terrestrial systems (e.g. via Hg deposition). Research indicates that fires are becoming more severe over much of North America, thus increasing element emissions during fire. However, there has been little research relating forest floor and mineral soil losses of C, N and Hg to on-the-ground indices of fire severity that enable scaling up those losses for larger-scale accounting of fire-level emissions. We investigated the relationships between forest floor and mineral soil elemental pools across a range of soil-level fire severities following the 2011 Pagami Creek wildfire in northern Minnesota, USA. We were able to statistically differentiate losses of forest floor C, N and Hg among a five-class soil-level fire severity classification system. Regression relationships using soil fire severity class were able to predict remaining forest floor C, N and Hg pools with 82–96% confidence. We correlated National Aeronautics and Space Administration Airborne Visible and Infrared Imaging Spectrometer-Classic imagery to ground-based plot-scale estimates of soil fire severity to upscale emissions of C, N and Hg to the fire level. We estimate that 468 000 Mg C, 11 000 Mg of N and over 122 g of Hg were emitted from the forest floor during the burning of the 28 310 ha upland area of the Pagami Creek fire.

Additional keywords: atmospheric pollutants, forest fire, global warming, greenhouse gases, nutrients.

Received 16 July 2016, accepted 17 February 2017, published online 30 March 2017

Introduction

Forest fires emit large amounts of C, N and Hg to the atmosphere (Amiro *et al.* 2001; Kasischke *et al.* 2005; Kolka *et al.* 2014). Globally, fires emit ~2 Pg of C annually to the atmosphere (van der Werf *et al.* 2010), which is comparable to 23% of total fossil fuel emissions (Boden *et al.* 2012). Similarly, fire results in an estimated 25 Tg of N or ~20% of anthropogenic emissions (Gruber and Galloway 2008), and ~675 Mg of Hg annually or 9% of all Hg emissions (Friedli *et al.* 2009). C and N emissions by fire increase atmospheric concentrations of greenhouse gases (van der Werf *et al.* 2010), possibly increasing climate forcing and global temperatures. Climate change is increasing drought and fire occurrence in the western USA (Westerling *et al.* 2006) and in the boreal region (Kelly *et al.* 2013), thus creating a positive feedback loop with emissions from fire. Generally, much of the C and N that is liberated during fire comes from the forest floor (or O-horizon) and in some cases the upper mineral layers of the soil (Nave *et al.* 2011;

Miesel *et al.* 2012). During fire, especially severe fire, organic matter pyrolysis affects the remaining structure and composition of soil organic matter, potentially having negative effects on nutrient cycling, soil water repellency and subsequent soil water status, and overall plant productivity (Neary *et al.* 1999). Losses of C and N can also increase the potential for erosion once the stabilising organic layer is consumed (Neary *et al.* 1999).

Hg is a pollutant of global concern because its organic form, methylmercury (MeHg), bioaccumulates in the food chain, leading to harmful effects on human nervous system functions (Scheuhammer *et al.* 2007). Fish consumption advisories for Hg are in place in all 50 states of the USA, all 13 Canadian provinces and territories, and across northern Europe and Australia, including global recommendations from the World Health Organization. Landscapes with a preponderance of lakes, streams and wetlands are especially vulnerable as MeHg is produced in low oxygen environments (Grigal 2003). The largest source of atmospheric Hg is the burning of fossil fuels and it is deposited as either wet or dry deposition (Witt *et al.* 2009; Pirrone *et al.* 2010). Hg emissions from uncontaminated soils are generally low and can even be negative as soils can be sinks for gaseous Hg (Haynes *et al.* 2017). Emissions of Hg during fire lead to increased local deposition downwind of fire as a result of particulate deposition. Studies in the sub-boreal region of northern Minnesota indicate Hg deposition resulting from fire can increase local annual deposition by 40% in the year of the fire (Witt *et al.* 2009), possibly leading to short-term increases in Hg in the aquatic food chain. However, losses of Hg from forest floor and mineral soils at the watershed scale following fire may reduce Hg in future upland hydrologic transport to surface waters, resulting in long-term decreases in Hg concentrations in the aquatic food chain (Gabriel *et al.* 2009).

As Hg has a high affinity for organic matter complexes, highest concentrations are found in upper soil layers where the most organic matter is present. Like C, Hg partitions between the solid and dissolved phase and complexes with humic acids and other dissolved phase fractions found in dissolved organic matter (Kerndorff and Schnitzer 1980). Numerous studies have shown relatively high correlations between Hg and dissolved organic C or dissolved organic matter in soils and surface waters (e.g. Kolka *et al.* 1999). During fire, both C and Hg are volatilised in gaseous forms, mainly CO_2 and Hg^0.

Fire severity and intensity are often wrongly used interchangeably. Keeley (2009) defines fire intensity as a measure of energy output, whereas fire severity or burn severity metrics indicate the loss or change in organic matter aboveground or below ground. Keeley (2009) also indicates that fire severity can be used to predict some ecosystem responses but not all. Jain and Graham (2007) used vegetation and soil data from Rocky Mountain fires to develop severity classes for both a tree fire severity index and soil fire severity index. Here we use the Jain *et al.* (2012) soil fire severity index to test for differences among classes in soil C, N and Hg pools and as a way to scale up elemental emissions to the fire scale.

High-severity fires oxidise soil organic matter and lead to decreases in overall soil C and N pools (Certini 2005); combined fire with blowdown and salvage logging (high fire severity) have been shown to decrease Hg forest floor pools (Mitchell *et al.* 2012). The ability to use fire severity as a surrogate for losses of forest floor and mineral soil C, N and Hg pools is needed to scale fire effects. Combining remote sensing techniques with on-the-ground data to test and validate larger-scale models is an important first step in being able use remote sensing to scale up emissions.

In our previous research on the Pagami Creek fire in northern Minnesota, we compared forest floor and mineral soil sampled at the scale of the forest floor frame (0.71 m^2; 30-cm diameter circular plots) to the Jain *et al.* (2012) soil fire severity index measured at 10-m^2 subplots and averaged at the plot scale (500 m^2; 25.2-m diameter circular plots). That approach failed to provide predictive relationships (Kolka *et al.* 2014), suggesting that the scale at which soil fire severity is determined is important for being able to identify relationships between soil fire severity and soil element response. Although our earlier research identified significant differences in forest floor pools of C, N and Hg between unburned and burned plots, it did not reveal differences among soil-level fire severity classes within the burned plots (Kolka *et al.* 2014). As a result, we conducted a second sampling 10 months after the Pagami Creek fire where we collected forest floor and mineral soils and soil fire severity information at the forest floor sampling frame scale on the same series of plots. Our two main objectives in this paper were to (1) distinguish C, N and Hg losses among soil fire severity classes at the scale of the forest floor frame, and (2) scale those losses to the fire scale by correlating remote sensing products with plot-scale estimates of soil fire severity. Being able to use soil fire severity to predict elemental emissions would represent a significant advancement in our ability to assess large-scale fire effects and recovery potential. This work was conducted using field data collected after the 2011 Pagami Creek wildfire in northern Minnesota, USA, which included both surface and crown fires, thus resulting in post-fire surface conditions that spanned the range of soil-level fire severity.

Materials and methods

Study site

The study was conducted within or immediately adjacent to the Superior National Forest in north-eastern Minnesota, USA (Fig. 1). The area has a mean annual precipitation of ~71 cm, and a mean annual temperature of 2°C, with mean July and January temperatures of 17°C and −8°C (Kolka *et al.* 2014). Undulating and glacially shaped terrain is underlain by Precambrian Canadian Shield bedrock, with soils formed primarily from glacial till and outwash resulting from the Rainy Lobe during the Wisconsin glacial episode. Upland soils are strongly influenced by variable depth to bedrock, and the landscape is embedded with abundant lakes and wetlands (Heinselman 1996). All upland mineral soils are Entisols or Inceptisols that are well drained and considered shallow with 20–50 cm of gravelly coarse sandy loam over bedrock; well drained with moderately deep (50–100 cm) gravelly sandy loam over bedrock; or well-drained deep soils >100 cm of gravelly sandy loam over bedrock. In the area of the fire, these broad soil categories are mainly based on depth to bedrock and each represent ~30–35% of the area (C. McQuiston, soil scientist, US Forest Service [USFS] Superior National Forest, pers. comm.).

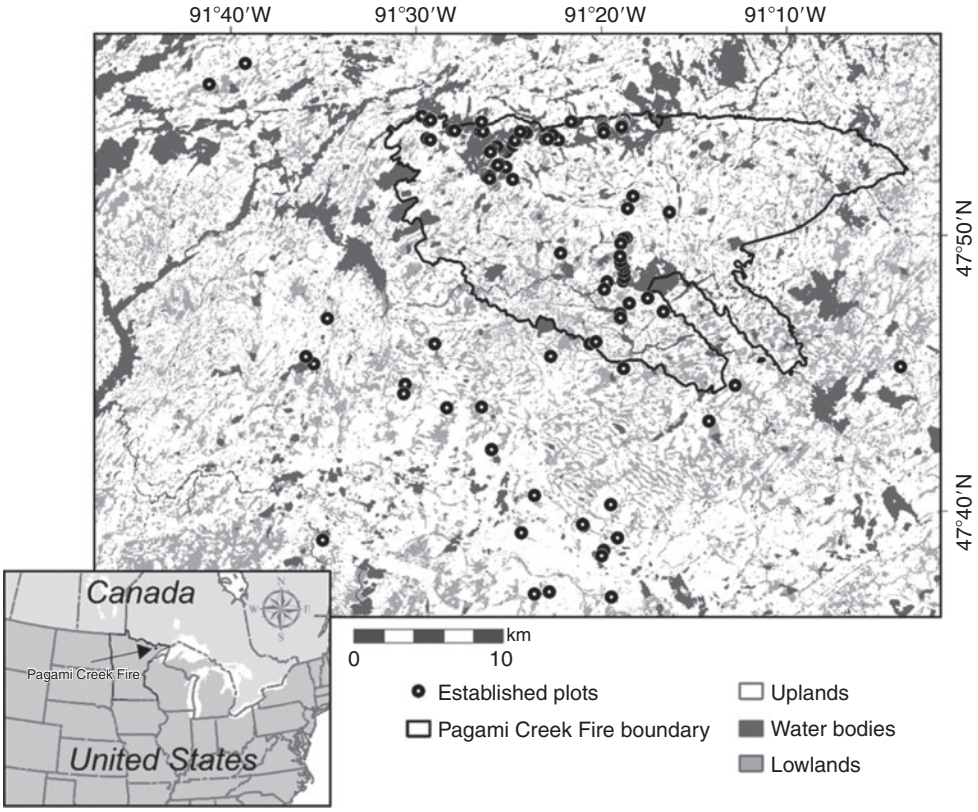

Fig. 1. Location of wildfire area and plot locations in north-eastern Minnesota, USA (Kolka *et al.* 2014).

The shallow-to-bedrock soils include Quetico (Lithic Udorthents) and Insula (Lithic Dystrudepts), and the moderately deep soils include Conic (Typic Dystrudepts) and Wahlsten (Oxyaquic Dystrudepts), with deep soils including Newfound (Typic Fragiudepts) (Soil Survey Staff 2010). Map units generally range from 2 to 18% slope with pines (e.g. *Pinus banksiana* Lamb. and *Pinus resinosa* Aiton) tending to be on shallow and sandier soils, deciduous species (e.g. *Populus tremuloides* Michx., *Populus grandidentata* Michx., *Betula papyrifera* Marshall, and *Acer rubrum* L.) on the deeper soils, and *Abies balsamea* (L.) Mill. and *Picea glauca* (Moench) Voss on the deepest and finest textured soils (C. McQuiston, pers. comm.).

A lightning strike on 18 August 2011 initiated a wildfire that began in the north-west corner of the Pagami Creek fire area (Fig. 1). The fire area grew slowly until 10 September when windy and dry conditions led to a blowup and the fire travelled 10 km to the south. A subsequent change in wind direction on 12 September pushed the fire an additional 30 km to the east and south-east. By late October 2011, the fire was contained after burning ~370 km^2, making it the largest fire in Minnesota since 1918 (Kolka *et al.* 2014).

Experimental design and soil collection

We designed our sampling for forest floor and mineral soil C, N and Hg pools based on pre- and post-fire satellite remote sensing data (relative differenced Normalised Burn Ratio algorithm [RdNBR; Miller *et al.* 2009]) and pre-fire maps of forest structure and composition that helped us identify areas likely to be more susceptible to higher-severity burns (Wolter *et al.* 2009; Wolter and Townsend 2011). Using the RdNBR and pre-fire maps we anticipated sampling across expected gradients in fire severity. Soils and ancillary data were collected during two periods. The first set of soil samples were collected in October–November 2011 and April–May 2012 with the data reported in Kolka *et al.* (2014). The October–November samples were collected immediately after the fire and focused on fire-affected plots. During this initial sampling campaign, it was apparent that our assessment of fire severity using remote sensing and pre-fire maps under-represented the highest soil fire severity classes. Therefore, additional soil samples were collected in April–May 2012 and included 24 unburned control plots established outside the Pagami Creek fire boundary, as well as 25 burned plots that represented the higher soil fire severity classes that were under-represented in the 2011 collection. The October–November 2011 and April–May 2012 samplings established 123, 12.6-m radius upland soil plots (wetland plots were excluded from this study), including the unburned control plots (Fig. 1, Kolka *et al.* 2014). The second sampling occurred in August–September 2012, ~10 months after the fire, and the data in this paper are based on the analysis of those samples. Even after 10 months, soil fire severity was easily estimated as regrowth was minimal. During the second sampling in August–September 2012, 102 of the original 123 plots were revisited and we collected triplicate forest floor and mineral samples at 4.2 m from the plot centre (0.5 m further from plot centre than the first sampling) at the

Fig. 2. Example of soil fire burn severity classes: (*a*) class 1, >85% forest floor remaining; (*b*) class 2, 40–85% forest floor remaining; (*c*) class 3, 1–40% forest floor remaining; and (*d*) class 4, 0% forest floor remaining.

same three cardinal directions (0°, 120° and 240°). Forest floor samples included the complete forest floor layer (litter + duff; i.e., complete organic horizon) collected within a 30-cm diameter circular sampling frame. Any apparent new litter (within the last 10 months) was removed from the forest floor sampling frame before collection of the complete forest floor layer. Following collection of the forest floor samples, forest floor depth was measured in the four cardinal directions (0°, 90°, 180° and 270°). Mineral soil samples were collected from 0–10 cm and 10–20-cm depths using a 5-cm diameter hammer-driven soil corer. As our initial results indicated few differences in C, N and Hg pools across soil fire severity classes when aggregated at the plot scale (Kolka *et al.* 2014), during the second sampling in August–September 2012, the forest floor and mineral soils were not aggregated and the soil fire severity was assessed within its respective forest floor sampling frame as described below.

Soil-level fire severity estimate

Jain and Graham (2007) developed a ground-based soil fire severity classification through a synthesis of the literature. The classification has five categories of soil fire severity ranging from 0 (unburned) to 4 (most severely burned). The soil fire severity class system corresponds to the post-fire index discussed by Jain *et al.* (2012), with the main class depending on the surface areal coverage of forest floor remaining (0–4 scale) and the subclass assessing the heat-induced oxidation level of the exposed mineral soils (i.e. colour, 0–3 scale). For the main class, 0 represents unburned, 1 represents the lightest burn class with >85% of the forest floor remaining, 2 represents areas with 40–85% forest floor remaining, 3 represents 1–40% forest floor remaining and 4 represents no forest floor remaining (see Fig. 2 for examples). Because of a small number of samples in some soil fire severity soil colour subclasses, we analysed the data at the top hierarchical severity class level (i.e. % of forest floor remaining, levels 0–4).

As described in Kolka *et al.* (2014), during the first soil sampling, soil fire severity was estimated on 10-m^2 circular subplots located at 6.5 m at three azimuths (0°, 120° and 240°) from plot centre that did not overlap where forest floor and mineral soil was sampled. The subplot soil fire severity components were averaged to the plot scale and compared with plot-aggregated forest floor and mineral soil C, N and Hg pools. For the data presented here, during the resample campaign in August–September 2012 we assessed soil-level fire severity within the 30-cm diameter forest floor sampling frame.

Soil analysis

Individual, non-aggregated forest floor and mineral soil samples from the August–September 2012 samples were frozen at −20°C upon return to the laboratory. Within 2 months, samples were thawed and a subsample was oven-dried at 65°C for forest floor and 105°C for mineral soils to measure and correct for soil moisture and subsequently to calculate bulk density. The remaining forest floor and mineral soil samples were air-dried and mineral soils were passed through a 2-mm sieve before grinding. Both forest floor and mineral soils were ground with a stainless steel Wiley mill with complete cleaning between samples. Samples were analysed for total C and N concentration

Table 1. Results of generalised linear models, showing *F* and *P* values for soil fire severity level for forest floor, 0–10 cm and 10–20-cm soil for C, N and Hg pools sampled in 2012 ($n = 236$).
Bold *P*-values are less than 0.05, indicating significance

Soil layer response variable		Severity level	
		F	*P*
Forest floor	C[A]	199.9	**<0.0001**
	N	202.7	**<0.0001**
	Hg	187.6	**<0.0001**
0–10-cm mineral	C[A]	1.24	0.2955
	N[A]	3.74	**0.0056**
	Hg[A]	1.12	0.3467
10–20-cm mineral	C[A]	3.15	**0.0152**
	N[A]	3.36	**0.0107**
	Hg[A]	3.02	**0.0188**

[A]Data were log-transformed before analysis.

on a LECO total elemental analyser with a separate subsample analysed for total Hg concentration using a direct Hg analyser (DMA-80, Milestone Inc.) and United States Environmental Protection Agency Method 7473 (USEPA 2009). To determine forest floor C, N and Hg mass per unit area (i.e. pools), we multiplied the C, N and Hg concentrations by the dry mass equivalent of the entire forest floor sample. For mineral soils the oven-dried corrected mass of the entire 0–10 and 10–20-cm depth increments were used to determine overall soil bulk density (including the >2-mm fraction). The fine soil bulk density (including only the <2-mm fraction) was determined following the removal of the >2-mm fraction, with the density of that fraction estimated to be 2.65 g cm^{-3} (i.e. the density of quartz). The pools of mineral soil C, N and Hg are based on the fine soil bulk density.

Statistical analyses

Here we analyse and report the results for the second soil sampling in August–September 2012. We determined variation in C, N and Hg pools across soil fire severity classes at the scale of the forest floor frame using one-way generalised linear models (PROC MIXED, SAS *v.* 9.3 Cary, NC) (Table 1). When differences among soil fire severity levels were significant, we performed mean separation tests using Tukey's adjustment for multiple comparisons (McDonald 2014).

To meet assumptions of normality, we log-transformed data for forest floor C pools, 0–10-cm mineral soil C, N and Hg pools and 10–20-cm mineral soil C, N and Hg pools before analysis. We ranked data for forest floor N and Hg pools before analysis because normality assumptions were not met for these variables under any standard transformations.

Scaling to upland fire-level emissions of C, N and Hg

National Aeronautics and Space Administration (NASA) Airborne Visible and Infrared Imaging Spectrometer-Classic (AVIRIS-C) imagery was collected over the study area 1 year after the fire (27–30 September 2012) from a Twin Otter aircraft flying at 5425 m above sea level (eight images total, ground resolution ~4 m). AVIRIS-C measures 350–2500 nm in nominal 10-nm wavebands (224 bands) with a signal-to-noise ratio greater than 500:1. AVIRIS-C data are provided by NASA-JPL orthorectified and atmospherically corrected to apparent at-surface reflectance (Thompson *et al.* 2015). Image preprocessing consisted of vector normalisation by pixel to remove the effects of cross-track illumination (due to the low solar angles) (e.g. Feilhauer *et al.* 2010). We utilised the minimum noise fraction (MNF) transform (Green *et al.* 1988; Boardman and Kruse 1994) for data dimensionality reduction and denoising. MNF transform is a two-part principal components analysis (PCA) transformation that first estimates the noise covariance matrix of the data and then uses the PCA of the noise-whitened image data to reduce the dimensionality of the imagery while simultaneously removing noise-dominated components. Like a classic PCA, bands showing the largest eigenvalues contain the most information, and bands showing progressively lower eigenvalues contain the 'noise components' of the imagery. The first five MNF bands showed substantial spatial and spectral variability within the burn scar and explained over 90% of the spectral variability in the imagery. These bands were extracted from MNF stacks of the images, resampled to 10-m resolution to reduce between-pixel heterogeneity, mosaicked into a single image and filtered with a 3 × 3-pixel moving window using a Gaussian averaging kernel. Subsequent statistical analyses utilised MNF bands 1–3 and 5 (band 4 was most strongly related to solar illumination gradients rather than fire effects). All water bodies and lowland forests were masked using data from Wolter *et al.* (2012) and the US Geological Survey National Land Cover Database 2011 land cover dataset (Homer *et al.* 2015). Image processing was conducted using ENVI (Exelis Visual Information Solutions, Broomfield, CO) and custom scripts written in the Interactive Data Language (IDL) and Python. AVIRIS-C MNF spectra were extracted for all plot locations, with locations falling within 10 m of water bodies or lowland forests masked from all analyses (final $n = 112$). We used a two-stage linear discriminant analysis (LDA) to classify (map) the Jain *et al.* (2012) soil fire severity classes (0–4) as a function of the four MNF bands. To refine and test the model, we utilised 1000 randomised permutations of the LDA split 60/40 into training and testing fractions stratified by the soil fire severity class. For the 1000 permutations, we assessed the percentage agreement between the mapped plot class and field-determined plot class (from the mean percentage organic matter cover of the three 10-m^2 subplots converted then to the Jain Index), labelled the observation based on the class it was mapped to 75% of the time, and then re-ran the LDA, again with 1000 permutations. A final model was then applied to the entire MNF dataset.

Results

Soil fire severity relationships with C, N and Hg pools

We found significant differences in forest floor C pools (Mg ha^{-1}) across all soil fire severity classes, and N (Mg ha^{-1}) and Hg (g ha^{-1}) pools significantly differed across all soil fire severity classes with the exception of the 0 and 1 classes, which were similar (Fig. 3). Forest floor C, N and Hg pools decreased with higher-severity fires. Our mean separation tests

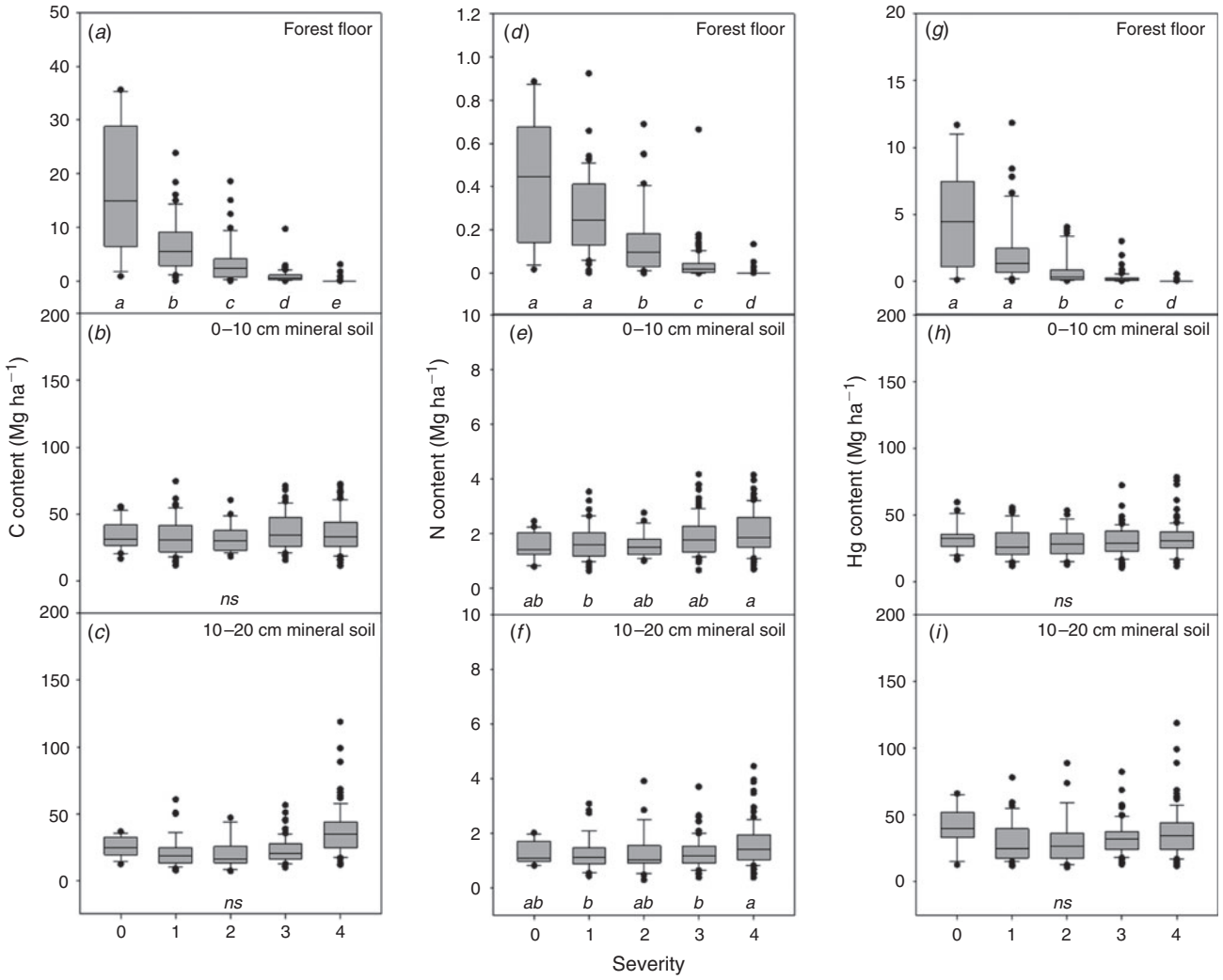

Fig. 3. Boxplots showing C, N and Hg pools in the forest floor (panels *a*, *d* and *g*), 0–10-cm mineral soil (panels *b*, *e* and *h*) and 10–20-cm mineral soil (panels *c*, *f* and *i*) by soil-level fire severity class for 2012 samples from the Pagami Creek wildfire. Italicised lowercase letters within panels indicate differences among soil fire severity levels at the $P \leq 0.05$ significance level, and 'ns' indicates no significant differences. Note differences in *y*-axis scales within and among elements.

failed to indicate statistically significant differences among soil fire severity classes for C and Hg pools in either the 0–10 or 10–20-cm mineral soils, probably as a result of the insulating ability of the forest floor. In contrast, at 0–10-cm soil depth, greater N pools were found in soil fire severity class 4 than in class 1, with other classes being similar. At 10–20-cm soil depth, greater N pools were found in soil fire severity class 4 than in class 1 and 3, with other classes being similar. Negative linear and exponential regression relationships for forest floor C, N and Hg pools with soil fire severity class were all highly significant (Table 2).

Table 2. Linear and exponential regression relationships between forest floor C, N (Mg ha^{-1}) and Hg (g ha^{-1}) pools and soil fire severity class ($P < 0.05$ for all regressions)

Element	Linear	R^2	Exponential	R^2
C	$C = -4.08(\text{class}) + 13.88$	0.82	$C = 25.37^{e^{-1.29(\text{class})}}$	0.94
N	$n = -0.11(\text{class}) + 0.51$	0.96	$n = 2.68^{e^{-1.21(\text{class})}}$	0.87
Hg	$Hg = -1.11(\text{class}) + 4.90$	0.86	$Hg = 36.65^{e^{-.48(\text{class})}}$	0.91

Remote sensing analyses

In the first-stage LDA, the majority (70%) of the original 112 locations (including only plots within the burn area; excluding some unburned plots outside the burn area) used for mapping showed no change in the assigned class between permutations. As described above, locations showing changes were assigned to classification present in >75% of the permutations, and the LDA was re-run producing final calibration and validation accuracies of 75.9% (±3.5% s.d.) and 69.6% (±4.6% s.d.). The two-stage analysis resulted in reductions of 25% and 23% in uncertainty from the first to second stage of analysis.

The image analyses indicated the upland area of the fire was ~28 310 ha with soil fire severity classes of 1 representing 9.5% of the area, 2 representing 4.2% of the area, 3 representing 23.9% of the area and 4 representing 62.4% of the area.

Losses of C, N and Hg pools at the fire scale

We scaled up the mean elemental differences between unburned forest floor and mineral soil samples and each of the burned soil fire severity classes by the area in each of the soil fire severity classes, to estimate fire-level emission losses. Based on differences in the forest floor element pools across soil fire severity classes, losses of C, N and Hg pools were estimated to be 468 000 Mg of C, 11 000 Mg of N and 122 kg of Hg over the 28 310 ha upland area of the Pagami Creek fire. Because of only mineral soil differences among the burned soil fire severity classes for N in the 0–10 and 10–20-cm pools (i.e. no difference between the unburned reference condition and burned classes), mineral soils did not contribute to fire-level losses of C, N and Hg.

Discussion

Our previous research in which we aggregated forest floor and mineral soils at the plot scale (25-m diameter) found elemental emission differences between the forest floor soil fire severity unburned class (0) and the burned classes (1–4), but no differences among the burned classes (Kolka *et al.* 2014). As a result, scaling of the losses of C, N and Hg pools to the fire scale was a mean of all burned soil fire severity classes. Results from the second sampling (August–September 2012), where we sampled and analysed forest floor and mineral soils without aggregation and conducted the soil fire severity classification at the scale of the forest floor frame, gave us greater ability to distinguish forest floor losses of C, N and Hg across the burned soil fire severity classes. The use of AVIRIS hyperspectral imagery to map Jain *et al.* (2012) soil fire severity classes further enabled us to scale the results to the whole fire with confidence. Our predictive capabilities captured almost 76% of the variation during model development and almost 70% during model validation. Forest floor pools of C, N and Hg measured at the scale of the forest floor frame were distinguishable across all soil fire severity classes with the exception of N and Hg pools between the unburned category (0) and lowest burn class (1). The lowest burn class is defined as having >85% surface cover of the forest floor remaining (Jain and Graham 2007); therefore, the difference between percentage forest floor remaining was least between the unburned (0) and lowest (1) severity class (i.e. 15%, whereas between classes 1 and 2 there is a 45% difference and between 2 and 3 there is a 40% difference, with class 4 at 0% forest floor remaining), possibly leading to more overlap in estimates of elemental pools between unburned and the lowest severity class, especially when considering burned areas can have up to 99% of the forest floor remaining.

For comparison, in boreal Alaska, a severity index (Composite Burn Index or CBI) was used to compare losses of organic layer C estimated by reconstructing the organic layer using the exposure of black spruce (*Picea mariana* (Mill.) B.S.P) adventitious roots following fire (Boby *et al.* 2010). When comparing the substrate component of the CBI to organic layer C combustion across 36 sites, Boby *et al.* (2010) found a fairly weak relationship ($R^2 = 0.28$). Using the same method across 81 burned sites in the boreal area of Alaska, Kasischke *et al.* (2008) found a similar weak relationship between substrate CBI and organic layer depth ($R^2 = 0.35$), and concluded that 'the CBI approach has limited potential for quantifying fire severity in these ecosystems, in particular organic layer consumption'. Boot *et al.* (2015) found no relationship between a three-class fire severity assessment and C pools in forest floor and upper mineral soils following fires in ponderosa pine (*Pinus ponderosa* Lawson & C. Lawson) ecosystems in Colorado, USA. In contrast to Boby *et al.* (2010), Kasischke *et al.* (2008) and Boot *et al.* (2015), using the Jain Index (Jain *et al.* 2012) we were able to develop very good relationships between soil fire severity index and elemental pools in the forest floor, with linear and exponential correlations ranging from 82 to 96% (Table 2). Mitchell *et al.* (2012) used a similar version of the classification as in this study and found a general pattern of higher forest floor Hg losses in higher-severity classes with no differences in mineral soils across severity classes. Using a fire severity classification suggested by Keeley (2009) that was a function of vegetation and surface soil effects, Woodruff and Cannon (2010) found differences between unburned and severely burned northern Minnesota sites in C and Hg from O+A-horizon soils, with a light–moderate burn severity class similar to both unburned and severely burned sites. Biswas *et al.* (2007) found differences in Hg storage in burned and unburned Rocky Mountain soils that appeared to include both organic and upper mineral soil horizons and inferred differences in Hg pools across three classes of fire severity, but the differences were not supported by statistical analyses. It is difficult to compare our results to those of Woodruff and Cannon (2010) and Biswas *et al.* (2007) because of the different approaches to soil sampling. A-horizon soil depth was generally shallow at our sites and given the large differences in forest floor (i.e. O-horizon) C, N and Hg pools, if combined we may have also seen differences. Engle *et al.* (2006) related mineral soil Hg losses following fire to C:Ca ratios as an indicator of fire severity (with lower C:Ca ratios being more severe), but found that the relationships were inconsistent. Acknowledging the work of Woodruff and Cannon (2010) and Mitchell *et al.* (2012), this is only one of a few studies to demonstrate that fire severity indices can produce statistically valid relationships that differentiate losses of forest floor C and Hg pools across soil fire severity classes, and the first study that has accomplished this for losses of N. Although fire effects on forested mineral soils vary, numerous studies have shown few effects on C and N pools in mineral soils (see reviews by Nave *et al.* 2011 and Miesel *et al.* 2012), which we attribute to the much more limited heating that is experienced in mineral soil layers, especially when forest floor cover persists to provide insulation to the underlying mineral soil (Neary *et al.* 2008).

In contrast to our results for 0–10 and 10–20-cm mineral soil C and Hg pools, we observed significant differences in N pools, with the highest soil fire severity class having the highest soil N pools among some of the burned classes, both at 0–10 cm and 10–20-cm soil depth. Others have found increases in soil N following fire and ascribe those differences to leaching of organically bound N from the remaining forest floor and ash,

and possibly biological fixation (Alban 1977; Lynham *et al.* 1998; Bodí *et al.* 2014).

In this study, forest floor emission rates ranged from 10 to 17 Mg ha^{-1} for C, 0.16–0.43 Mg ha^{-1} for N and 2.5–4.6 g ha^{-1} for Hg across the four soil fire severity burn classes. Our results fall within or close to the range that Boby *et al.* (2010) found for organic soil C (10–40 Mg ha^{-1}) and N (0.25–1.3 Mg ha^{-1}) for boreal forest fires in Alaska. Also within the range of our Hg emissions, Engle *et al.* (2006) found emissions of 2.6 and 3.6 g ha^{-1} for Hg for wildfire and prescribed fire for forest fires in the Sierra Nevada. Homann *et al.* (2015) found generally higher Hg emissions for forest wildfires in south-western Oregon in unthinned, thinned and clearcut sites (~4.5, 18 and 20 g ha^{-1}). Hg emissions from the unthinned site were from the forest floor only and were comparable to emissions for our highest soil fire severity burn class (4.6 g ha^{-1}), while both thinned and clearcut sites also had losses from upper mineral soils (A horizon) leading to higher Hg emissions. Similarly, Carpi *et al.* (2014) used chamber methods to measure Hg fluxes of 4.1 g ha^{-1} from Brazilian forest soils (0–5 cm) during harvesting and fire that also fall into the range we measured.

The relationship between forest floor element losses and soil fire severity both assessed at the scale of the forest floor frame, combined with remotely sensed assessments of plot-scale soil fire severity, allowed us to extrapolate post-fire elemental losses for the entire burn area. Overall, we estimate a 94% decrease in the forest floor C pool as a result of the fire that led to 468 000 Mg of C emissions; a decrease of 90% in the forest floor N pool that led to 11 000 Mg of N emissions; and a 94% decrease in forest floor Hg that lead to emissions of 122 g of Hg. These estimates are more reliable than previous estimates from Kolka *et al.* (2014) (~500 000 Mg of C, 5000 Mg of N and 250 g of Hg) that used the difference between unburned reference systems and the average of all the burned classes, because differences among soil fire severity classes were not detected when aggregated samples were used in relation to plot-level soil fire severity assessments. Given the importance of forest fires on global budgets of greenhouse gases (notably CO_2, CO, CH_4, N_2O, NO_x), ecosystem N fertilisation and the health implications of Hg, it is valuable to use remote sensing approaches to model emissions at various scales for greenhouse gas accounting, and understanding ecosystem N dynamics and sources and deposition of Hg. Considering the widespread nature of fires and that they often occur in very remote areas, the potential to use remote sensing to estimate C, N and Hg emissions from spectral data is an important advance. Others have used large-scale remote sensing of fire severity to scale up elemental losses from fire (Friedli *et al.* 2009; Barrett *et al.* 2010; van der Werf *et al.* 2010; French *et al.* 2011), but these studies did not use field-verified relationships with fire severity to make larger-scale assessments. In a similar context, Santín *et al.* (2015) used remote sensing to map fire severity following fires in eucalypt forests in Australia and found significant increases in the amount of ash when comparing low to high, and high to extreme fire severity. Elemental analyses of the ash samples included C, N and Hg (among many others) with no differences in concentrations between severity classes for N and Hg, with C concentration highest for the low severity class and no difference between high and extreme classes (Santín *et al.* 2015). Their motivation was to determine possible elemental loading to surface waters resulting from ash transport during erosion (Santín *et al.* 2015). We are not aware of any other studies that have used field-verified relationships between fire severity and elemental pools to scale up losses of emissions from forest fires.

Conclusions

Soil-level fire severity classification was successfully used to differentiate losses of C, N and Hg pools from forest floor 10 months after the Pagami Creek fire. Relationships were developed between element pools and soil fire severity classes by assessing fire severity at the same scale as our forest floor (and mineral soil) sampling. Using remotely sensed estimates of soil-level fire severity at the plot scale, we were then able to scale up C, N and Hg losses as a result of the Pagami Creek fire. This suggests great potential for using imaging spectroscopy data as a basis to scale elemental fluxes based on mapped fire severity. Taken together, our results suggest that future research aimed at scaling post-fire losses of forest floor and mineral soil C, N and Hg should combine small-scale soil sampling and severity measurements with large-scale remotely sensed assessments of fire severity to scale up emission losses.

Acknowledgements

This research was funded through the National Science Foundation grant DEB-1201484, NASA's Terrestrial Ecology Program for AVIRIS image acquisition, the USDA Forest Service Northern Research Station, and the USDA Forest Service National Fire Plan. We wish to thank the Superior National Forest staff (especially Bruce Anderson, Jim Saunders, Patti Johnson, Heather Jensen and Tom McCann) for their coordination and assistance that made this study possible. A special thanks to Terry Jain for her guidance in applying the soil severity index, and Mike Reinikainen for his assistance with classifying burn components. We also thank the many field personnel who assisted with the field campaign (Joel Flory, Alex Brito, Rob Focht, Jason Sedin, Amy Milo, Heather Fox, Bernard Isaacson, Clayton Kingdon, Donna Olson, Rayma Cooley, Bert Hyde, Johnna Hyde, Eric Gustafson, Dan Baumann, Hans Casperson, Daina Antanaitis, Holly Havanek, Hannah Manninen, Hannah Hubanks, Scott Brennan and Arjan DeBruijn), Robi Phetteplace and Clayton Kingdon, who assisted with the photo classification, Sue Lietz for soil severity data analyses and the creation of Fig. 1 and Kevin Horsager for assisting with sample analysis.

References

Alban DH (1977) Influence on soil properties of prescribed burning under mature red pine. USDA Forest Service, North Central Research Station, Research Paper NC-139. (St Paul, MN)

Amiro BD, Todd JB, Wotton BM, Logan KA, Flannigan MD, Stocks BJ, Mason JA, Martell DL, Hirsch KG (2001) Direct carbon emissions from Canadian forest fires, 1959 to 1999. *Canadian Journal of Forest Research* **31**, 512–525. doi:10.1139/X00-197

Barrett K, Kasischke ES, McGuire AD, Turetsky MR, Kane ES (2010) Modeling fire severity in black spruce stands in the Alaskan boreal forest using spectral and non-spectral geospatial data. *Remote Sensing of Environment* **114**, 1494–1503. doi:10.1016/J.RSE.2010.02.001

Biswas A, Blum JD, Klaue B, Keeler JG (2007) Release of mercury from Rocky Mountain forest fires. *Global Biogeochemical Cycles* **21**, GB1002. doi:10.1029/2006GB002696

Boardman JW, Kruse FA (1994) Automated spectral analysis: a geological example using AVIRIS data, north Grapevine Mountains, Nevada: In 'Proceedings, ERIM 10th thematic conference on geologic remote

sensing', 9–12 May 1994, San Antonio, TX, pp. I-407–I-418. Environmental Research Institute of Michigan (Ann Arbor, MI)

Boby LA, Schuur EAG, Mack MC, Verbyla D, Johnstone JF (2010) Quantifying fire severity, carbon, and nitrogen emissions in Alaska's boreal forest. *Ecological Applications* **20**, 1633–1647. doi:10.1890/08-2295.1

Boden TA, Marland G, Andres RJ (2012) Global, regional, and national fossil-fuel CO_2 emissions. US Department of Energy, Carbon Dioxide Information Analysis Center, Oak Ridge National Laboratory (Oak Ridge, TN). doi:10.3334/CDIAC/00001_V2012

Bodí MB, Martin DA, Balfour VN, Santín C, Doerr SH, Pereira P, Cerdà A, Mataix-Solera J (2014) Wildland fire ash: production, composition and eco-hydro-geomorphic effects. *Earth-Science Reviews* **130**, 103–127. doi:10.1016/J.EARSCIREV.2013.12.007

Boot CM, Haddix M, Paustian K, Cotrufo MF (2015) Distribution of black carbon in ponderosa pine forest floor and soils following the High Park wildfire. *Biogeosciences* **12**, 3029–3039. doi:10.5194/BG-12-3029-2015

Carpi A, Fostier AH, Orta OR, dos Santos JC, Gittings M (2014) Gaseous mercury emissions from soil following forest loss and land use changes: field experiments in the United States and Brazil. *Atmospheric Environment* **96**, 423–429. doi:10.1016/J.ATMOSENV.2014.08.004

Certini G (2005) Effects of fires on properties of forest soil: a review. *Oecologia* **143**, 1–10. doi:10.1007/S00442-004-1788-8

Engle MA, Gustin MS, Johnson DW, Murphy JF, Miller WW, Walker RF, Wright J, Markee M (2006) Mercury distribution in two Sierran forest and one desert sagebrush steppe ecosystems and the effects of fire. *The Science of the Total Environment* **367**, 222–233. doi:10.1016/J.SCITOTENV.2005.11.025

Feilhauer H, Asner GP, Martin RE, Schmidtlein S (2010) Brightness-normalized partial least squares regression for hyperspectral data. *Journal of Quantitative Spectroscopy & Radiative Transfer* **111**, 1947–1957. doi:10.1016/J.JQSRT.2010.03.007

French NHF, de Groot WJ, Jenkins LK, Rogers BM, Alvarado E, Amiro B, de Jong B, Goetz S, Hoy E, Hyer E, Keane R, Law BE, McKenzie D, McNulty SG, Ottmar R, Pérez-Salicrup DR, Randerson J, Robertson KM, Turetsky M (2011) Model comparisons for estimating carbon emissions from North American wildland fire. *Journal of Geophysical Research* **116**, G00K05. doi:10.1029/2010JG001469

Friedli HR, Arellano AF, Cinnirella S, Pirrone A (2009) Initial estimates of mercury emissions to the atmosphere from global biomass burning. *Environmental Science & Technology* **43**, 3507–3513. doi:10.1021/ES802703G

Gabriel MC, Kolka R, Wickman T, Nater E, Woodruff L (2009) Evaluating the spatial variation of total mercury concentrations in young-of-year fish for watershed-lake systems within the southern Boreal Shield. *The Science of the Total Environment* **407**, 4117–4126. doi:10.1016/J.SCITOTENV.2009.03.019

Green AA, Berman M, Switzer P, Craig MD (1988) A transformation for ordering multispectral data in terms of image quality with implications for noise removal. *IEEE Transactions on Geoscience and Remote Sensing* **26**(1), 65–74. doi:10.1109/36.3001

Grigal D (2003) Mercury sequestration in forests and peatlands. *Journal of Environmental Quality* **32**, 393–405. doi:10.2134/JEQ2003.3930

Gruber N, Galloway JN (2008) An Earth-system perspective of the global nitrogen cycle. *Nature* **451**, 293–296. doi:10.1038/NATURE06592

Haynes KM, Kane E, Potvin L, Lilleskov E, Kolka RK, Mitchell CPJ (2017) Gaseous mercury fluxes in peatlands and the potential influence of climate change. *Atmospheric Environment* **154**, 247–259. doi:10.1016/J.ATMOSENV.2017.01.049

Heinselman ML (1996) 'The Boundary Waters wilderness ecosystem.' (University of Minnesota Press: Minneapolis, MN)

Homann PS, Darbyshire RL, Bormann BT, Morrissette BA (2015) Forest structure affects soil mercury losses in presence and absence of wildfire. *Environmental Science & Technology* **49**, 12714–12722. doi:10.1021/ACS.EST.5B03355

Homer CG, Dewitz JA, Yang L, Jin S, Danielson P, Xian G, Coulston J, Herold ND, Wickham JD, Megown K (2015) Completion of the 2011 National Land Cover Database for the conterminous United States – representing a decade of land cover change information. *Photogrammetric Engineering and Remote Sensing* **81**(5), 345–354.

Jain TB, Graham RT (2007) The relation between tree burn severity and forest structure in the Rocky Mountains. In 'Restoring fire-adapted ecosystems: proceedings of the 2005 National Silviculture Workshop', 6–10 June 2005, Tahoe City, CA. (Ed. RF Powers) USDA Forest Service, Pacific Southwest Research Station, General Technical Report PSW-GTR-203, pp. 213–250. (Albany, CA)

Jain TB, Pilliod DS, Graham RT, Lentile LB, Sandquist JE (2012) Index for characterizing post-fire soil environments in temperate coniferous forests. *Forests* **3**, 445–466. doi:10.3390/F3030445

Kasischke E, Hyer EJ, Novelli P, Bruhwiler L, French NHF, Sukhinin AI, Hewson JH, Stocks BJ (2005) Influences of boreal fire emissions on Northern Hemisphere atmospheric carbon and carbon monoxide. *Global Biogeochemical Cycles* **19**, GB1012. doi:10.1029/2004GB002300

Kasischke ES, Turetsky MR, Ottmar RD, French NHF, Hoy EE, Kane ES (2008) Evaluation of the composite burn index for assessing fire severity in Alaskan black spruce forests. *International Journal of Wildland Fire* **17**, 515–526. doi:10.1071/WF08002

Keeley JE (2009) Fire intensity, fire severity and burn severity: a brief review and suggested usage. *International Journal of Wildland Fire* **18**, 116–126. doi:10.1071/WF07049

Kelly R, Chipman ML, Higuera PE, Stefanova I, Brubaker LB, Hu FS (2013) Recent burning of boreal forests exceeds fire regime limits of the past 10,000 years. *Proceedings of the National Academy of Sciences of the United States of America* **110**, 13055–13060. doi:10.1073/PNAS.1305069110

Kerndorff H, Schnitzer M (1980) Sorption of metals on humic acid. *Geochimica et Cosmochimica Acta* **44**, 1701–1708. doi:10.1016/0016-7037(80)90221-5

Kolka RK, Grigal DF, Verry ES, Nater EA (1999) Mercury and organic carbon relationships in streams draining forested upland/peatland watersheds. *Journal of Environmental Quality* **28**(3), 766–775. doi:10.2134/JEQ1999.00472425002800030006X

Kolka R, Sturtevant B, Townsend P, Miesel J, Wolter P, Fraver S, DeSutter T (2014) Forest floor and upper mineral soil carbon, nitrogen and mercury pools shortly after fire and comparisons utilizing fire severity indices. *Soil Science Society of America Journal* **78**(S1), S58–S65. doi:10.2136/SSSAJ2013.08.0351NAFSC

Lynham TJ, Wickware GM, Mason JA (1998) Soil chemical changes and plant succession following experimental burning in immature jack pine. *Canadian Journal of Soil Science* **78**, 93–104. doi:10.4141/S97-031

McDonald JH (2014) 'Handbook of biological statistics', 3rd edn. (Sparky House Publishing: Baltimore, MD).

Miesel J, Goebel PC, Corrace RG, Hix D, Kolka R, Palik B, Mladenoff D (2012) Fire effects on soils in Lake States forests: a compilation of published research to facilitate long-term investigations. *Forests* **3**, 1034–1070. doi:10.3390/F3041034

Miller JD, Knapp EE, Key C, Skinner CN, Isbell CJ, Creasy RM, Sherlock JW (2009) Calibration and validation of the relative differenced Normalized Burn Ratio (RdNBR) to three measures of fire severity in the Sierra Nevada and Klamath Mountains, California, USA. *Remote Sensing of Environment* **113**, 645–656. doi:10.1016/J.RSE.2008.11.009

Mitchell CPJ, Kolka RK, Fraver S (2012) The singular and combined effects of blowdown, salvage logging and wildfire on forest floor and soil mercury pools. *Environmental Science & Technology* **46**, 7963–7970. doi:10.1021/ES300133H

Nave LE, Vance ED, Swanston CW, Curtis PS (2011) Fire effects on temperate forest soil C and N storage. *Ecological Applications* **21**, 1189–1201. doi:10.1890/10-0660.1

Neary DG, Klopatek CC, DeBano LF, Ffolliott PF (1999) Fire effects on belowground sustainability: a review and synthesis. *Forest Ecology and Management* **122**, 51–71. doi:10.1016/S0378-1127(99)00032-8

Neary DG, Ryan KC, DeBano LF (2008) Wildland fire in ecosystems: effects of fire on soils and water. USDA Forest Service, Rocky Mountain Research Station, General Technical Report, RMRS-GTR-42-vol.4. (Ogden, UT).

Pirrone N, Cinnirella S, Feng X, Finkelman RB, Friedli HR, Leaner J, Mason R, Mukherjee AB, Stracher GB, Streets DG, Telmer K (2010) Global mercury emissions to the atmosphere from anthropogenic and natural sources. *Atmospheric Chemistry and Physics* **10**, 5951–5964. doi:10.5194/ACP-10-5951-2010

Santín C, Doerr SH, Otero XL, Chafer CJ (2015) Quantity, composition and water contamination potential of ash produced under different wildfire severities. *Environmental Research* **142**, 297–308. doi:10.1016/J.ENVRES.2015.06.041

Scheuhammer AM, Meyer MW, Sandheinrich MB, Murray MW (2007) Effects of environmental methylmercury on the health of wild birds, mammals and fish. *Ambio* **36**, 12–19. doi:10.1579/0044-7447(2007)36[12:EOEMOT]2.0.CO;2

Soil Survey Staff (2010) 'Key to soil taxonomy', 11th edn. (USDA Natural Resource Conservation Service: Washington, DC)

Thompson DR, Gao B-C, Green RO, Roberts DA, Dennison PE, Lundeen SR (2015) Atmospheric correction for global mapping spectroscopy: ATREM advances for the HyspIRI preparatory campaign. *Remote Sensing of Environment* **167**, 64–77. doi:10.1016/J.RSE.2015.02.010

USEPA (2009) Method 7473: mercury in solids and solutions by thermal decomposition, amalgamation, and atomic adsorption spectrophotometry. Available at http://www.epa.gov/wastes/hazard/testmethods/sw846/pdfs/7473.pdf [Verified 17 September 2014]

van der Werf GR, Randerson JT, Giglio L, Collatz GJ, Mu M, Kasibhatla PS, Morton DC, DeFries RS, Jin Y, van Leeuwen TT (2010) Global fire emissions and the contribution of deforestation, savanna, forest, agricultural, and peat fires (1997–2009). *Atmospheric Chemistry and Physics* **10**, 11707–11735. doi:10.5194/ACP-10-11707-2010

Westerling AL, Hidalgo HG, Cayan DR, Swetnam DW (2006) Warming and earlier spring increase Western U.S. forest wildfire activity. *Science* **313**, 940–943. doi:10.1126/SCIENCE.1128834

Witt EL, Kolka RK, Nater EA, Wickman TR (2009) Forest fire effects on mercury deposition in the boreal forest. *Environmental Science & Technology* **43**, 1776–1782. doi:10.1021/ES802634Y

Wolter PT, Townsend PA (2011) Estimating forest species composition using a multi-sensor fusion approach. *Remote Sensing of Environment* **115**, 671–691. doi:10.1016/J.RSE.2010.10.010

Wolter PT, Townsend PA, Sturtevant BR (2009) Estimation of forest structural parameters using 5 and 10 meter SPOT-5 satellite data. *Remote Sensing of Environment* **113**, 2019–2036. doi:10.1016/J.RSE.2009.05.009

Wolter PT, Sturtevant BR, Miranda BR, Lietz SM, Townsend PA, Pastor J 2012. Forest land cover change (1975–2000) in the Greater Border Lakes region. USDA Forest Service, Northern Research Station. Research Map NRS-3. (Newtown Square, PA).

Woodruff LG, Cannon WF (2010) Immediate and long-term fire effects on total mercury in forest soils of northeastern Minnesota. *Environmental Science & Technology* **44**, 5371–5376. doi:10.1021/ES100544D